Skeletal Scintigraphy: General Considerations

15

S. Ted Treves

Skeletal scintigraphy provides a functional image of bone. It is a highly sensitive method that depicts early changes in bone flow and turnover. Because of this high sensitivity, skeletal scintigraphy allows early diagnosis of disease often days or weeks before disease can be visualized on anatomic imaging. Therefore, skeletal scintigraphy assists in establishing early treatment and hopefully achieving better patient outcomes. However, as with other nuclear medicine imaging procedures, this high sensitivity is generally accompanied by a low level of specificity. Information about early changes in blood flow and bone turnover cannot be obtained, or not easily obtained, by other imaging methods. Although the spatial resolution of bone scintigraphy is relatively low compared to anatomic imaging, one can say that its functional resolution is very high.

Skeletal development and remodeling are integral parts of the physiology of bone. As the patient grows and develops, bone undergoes constant remodeling. Immature bone (woven bone) is replaced by mature lamellar bone. A skeletal scintigram can be considered not just as a static image but also as a "snapshot" of an ongoing dynamic process. As such, the bone scan can be thought of as a "slow dynamic" study. Approximately 10 % of the entire adult skeleton is replaced every year. Remodeling is, in great part, a functional adaptation of bone to the forces or stresses of daily life. When interpreting pediatric skeletal scintigraphy, it is important to keep in mind the characteristic patterns of pediatric skeletal growth and development and learn to recognize these patterns so they can be distinguished from actual lesions. The distribution of bone-seeking radiopharmaceuticals varies with age and with the activity of growth centers. It is necessary for growth centers to be ossifying in order for bone-seeking radiopharmaceuticals to be taken up in these regions. Otherwise, the center will appear devoid of activity. Ossification of growth centers occurs at different ages until all close by approximately 25 years of age. During the first year of life until 5 years of age, secondary ossification centers appear in the epiphysis. From 5 to 14 years of age, ossification rapidly spreads from the ossification centers, and various bones become ossified. The upper limbs and the scapula become ossified by 17–20 years. The bones of the lower limbs and the os coxae completely ossify by ages 18–23. By ages 23–25, the sternum, clavicles, and vertebrae become completely ossified. There may or may not be direct correlation between the radiographic and scintigraphic appearance of growth centers. Examples of absent-to-reduced tracer uptake in growth centers include the femoral head,

S.T. Treves, MD
Joint Program in Nuclear Medicine,
Department of Radiology, Harvard Medical School,
Boston, MA, USA

Division of Nuclear Medicine and Molecular Imaging, Department of Radiology,
Boston Children's Hospital,
Boston, MA, USA

Division of Nuclear Medicine and Molecular Imaging, Department of Radiology,
Brigham and Women's Hospital, Boston, MA, USA
e-mail: ted_treves@HMS.harvard.edu

S.T. Treves (ed.), *Pediatric Nuclear Medicine and Molecular Imaging*,
DOI 10.1007/978-1-4614-9551-2_15,

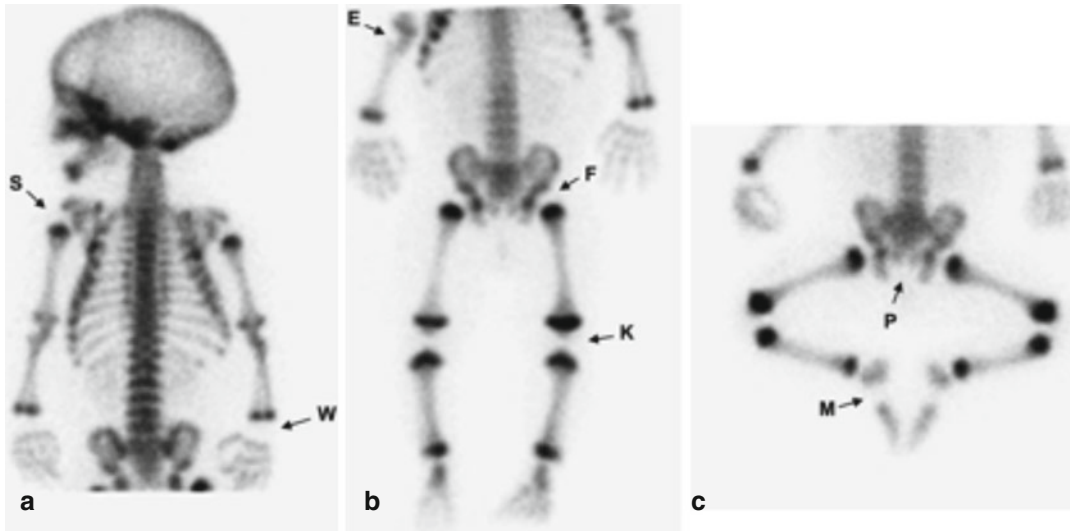

Fig. 15.1 (**a**–**c**) Absent tracer uptake in non-ossified centers. *S* shoulder, *W* wrist, *E* elbow, *F* femoral head, *K* knee, *P* pubis, *M* mid-foot

Fig. 15.2 Bilateral open ischiopubic synchondrosis (*arrows*)

Table 15.1 Indications for skeletal scintigraphy in children

Osteomyelitis
Chronic recurrent multifocal osteomyelitis (CRMO)
Sports injuries
Back pain
Avulsion fractures
The limping child. Toddler's injuries
Localization of the source of pain
Non-accidental trauma
Avascular necrosis of bone
Benign tumors (osteoid osteoma)
Bone infarction
Cysts
Fibrous dysplasia
Bone island
Hemangioma
Langerhans cell histiocytosis
Hyperostosis oncologic disorders (osteosarcoma, Ewing's sarcoma, rhabdomyosarcoma)
Radiation injury

the patella, the tarsal navicular, and the ischiopubic synchondrosis. During ossification, the ischiopubic synchondrosis can show focal increased tracer uptake which can be unilateral or bilateral, and this appearance should not be confused with a lesion (Figs. 15.1 and 15.2).

Whether a lesion is detected on conventional anatomic imaging depends on the degree of bone loss or deposition and on the stage of development of the lesion. For example, when excessive force is applied to a bone, or a lesion affects the bone, the bone reacts by forming new and stronger bone. In this early phase, anatomic imaging may not detect the abnormality unless significant bone loss has developed. Initially, the region of bone exposed to such force shows increased regional blood flow, which is part of the process of bone remodeling. During the process of bone remodeling, the bone is rather weak and vulnerable to further injury. Focal or diffuse increased blood flow can be seen on radionuclide angiography and on immediate (tissue) images as well as on skeletal images as regions of increased tracer concentration. Bone remodeling accompanied by increased tracer

uptake can go on for a period of time and depends on the progress stage of the lesion. Increased tracer uptake can persist, can become less noticeable, or can even disappear, and the bone scan may appear normal. For example, a bone scan may, at the end, appear normal in the presence of a well-established bone lesion. As an example, in an old spondylolytic lesion where the bone has become "quiescent" (doesn't show increased blood flow or high bone turnover), the bone scan may not demonstrate a focal abnormality, while anatomic imaging will likely show the fracture. Pediatric indications for skeletal scintigraphy that include benign and oncologic disorders are listed in Table 15.1. In the assessment of children with lower extremity or back pain, consider the benefit of large area imaging easily available with ^{99m}Tc-MDP scintigraphy or ^{18}F-NaF PET in the diagnosis and localization of pain of skeletal origin. This concept is applicable anywhere in the body. Children (and sometime adults) may have trouble identifying the source of pain. Pain may be referred to region distant from the site of a bone lesion. Some patients have conventional imaging focusing on a small area, which is clinically thought to be the source of pain. This approach may miss a skeletal source of pain. Therefore, one should keep in mind the benefit of skeletal scintigraphy evaluating a large area that goes beyond the reported symptom. A useful approach would be as follows: once an abnormality is identified on scintigraphy, anatomic imaging can be focused to the area of interest and help provide a higher level of diagnostic specificity (Fig. 15.3).

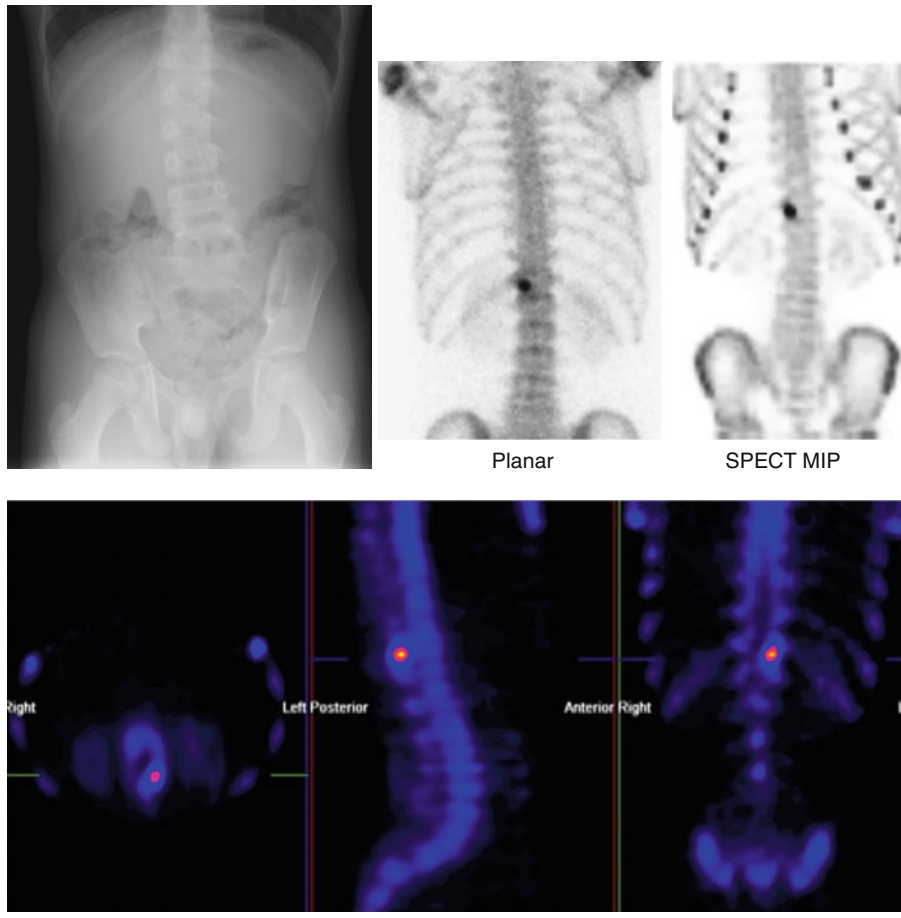

Fig. 15.3 An 11-year-old male with low back pain for several months. Relieved by Advil. X-ray suggested scoliosis. New plain x-rays suggested sclerosis of pedicle of L5. Bone SPECT showed intense and focal increased tracer uptake at T12. Finding suggested osteoid osteoma. A repeat CT showed findings compatible to an osteoid osteoma at T12

Fig. 15.3 (continued)

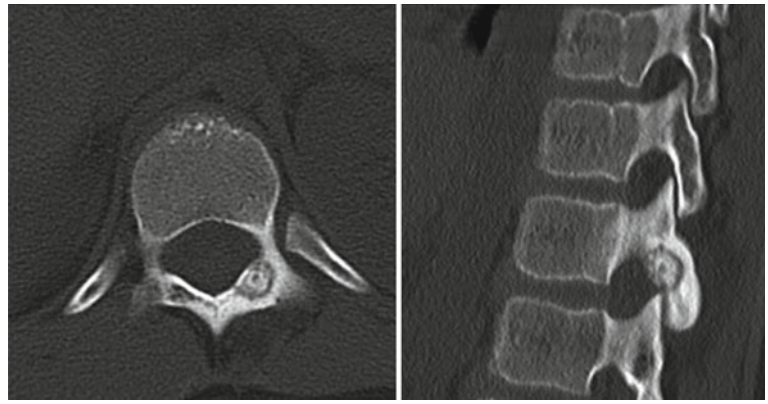

CT

Fig. 15.4 Vascular tamponade. Pinhole ^{99m}Tc-MDP images of the right hip from an 11-month-old with a tense hip effusion producing vascular tamponade of the femoral head. There is absent tracer uptake in the femoral head (*left image*). A follow-up image after the patient's effusion was drained reveals return of flow to the femoral head as evidenced by tracer uptake in it (*right image*)

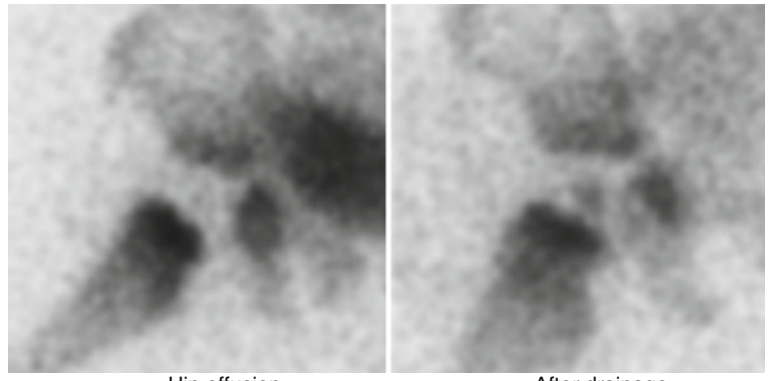

Hip effusion After drainage

Radiopharmaceuticals

Technetium-99m-MDP

Technetium-99m-MDP is the most commonly used radiopharmaceutical for skeletal scintigraphy. It is easily prepared in the nuclear medicine department from a kit, or it can be obtained already prepared and calibrated from commercial radiopharmacies. Following intravenous injection of ^{99m}Tc-MDP, skeletal distribution and uptake of this agent depend on regional blood flow and bone turnover. On skeletal scintigraphy, regions of reduced-to-absent blood flow will be seen as regions of reduced-to-absent tracer uptake (e.g., in a tense hip effusion or in the femoral head after a femoral neck fracture) (Figs. 15.4 and 15.5).

Hip effusion can occur without compromising perfusion of the femoral head (Fig. 15.6). Disuse of an extremity, for example, after a fall, can cause relatively decreased tracer uptake in the extremity not bearing weight even for a few days. Conversely, the contralateral extremity that bears weight will show relatively increased tracer uptake owing to the relatively increased blood flow to such extremity (Fig. 15.7).

In bone infarction such as in sickle cell disease, blood flow to the area involved is significantly reduced or absent. In this case, tracer delivery and bone uptake will be reduced to absent (Fig. 15.8).

Elegant autoradiography studies by Tilden et al. revealed that ^{99m}Tc-phosphates localize in lines between osteoid lining marrow cavities and the more peripheral bone (Fig. 15.9) [1]. After intravenous injection, blood activity levels fall to 4–10 % of the administered dose by 2 h and down to 3–5 % in 3 h. Less than 2 % of the activity is in the blood by 24 h after administration. Approximately 30 % of the activity is

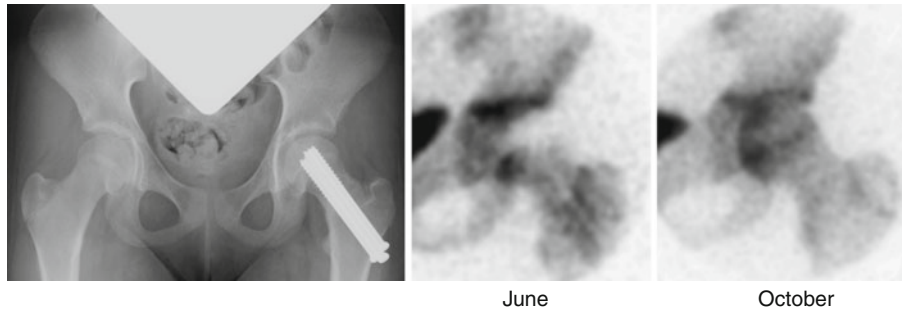

Fig. 15.5 Avascular femoral head and reperfusion after treatment. A 12-year-old girl with a left femoral neck fracture. Metallic pins (*left*) were inserted under an open reduction internal fixation (ORIF), and the initial ^{99m}Tc-MDP pinhole image (*center*) obtained soon after the surgery shows lack of vascularity in the femoral head as well as the defects corresponding to the metallic pins. A similar image obtained 4 months after surgery (*right*) reveals reperfusion of the left femoral head

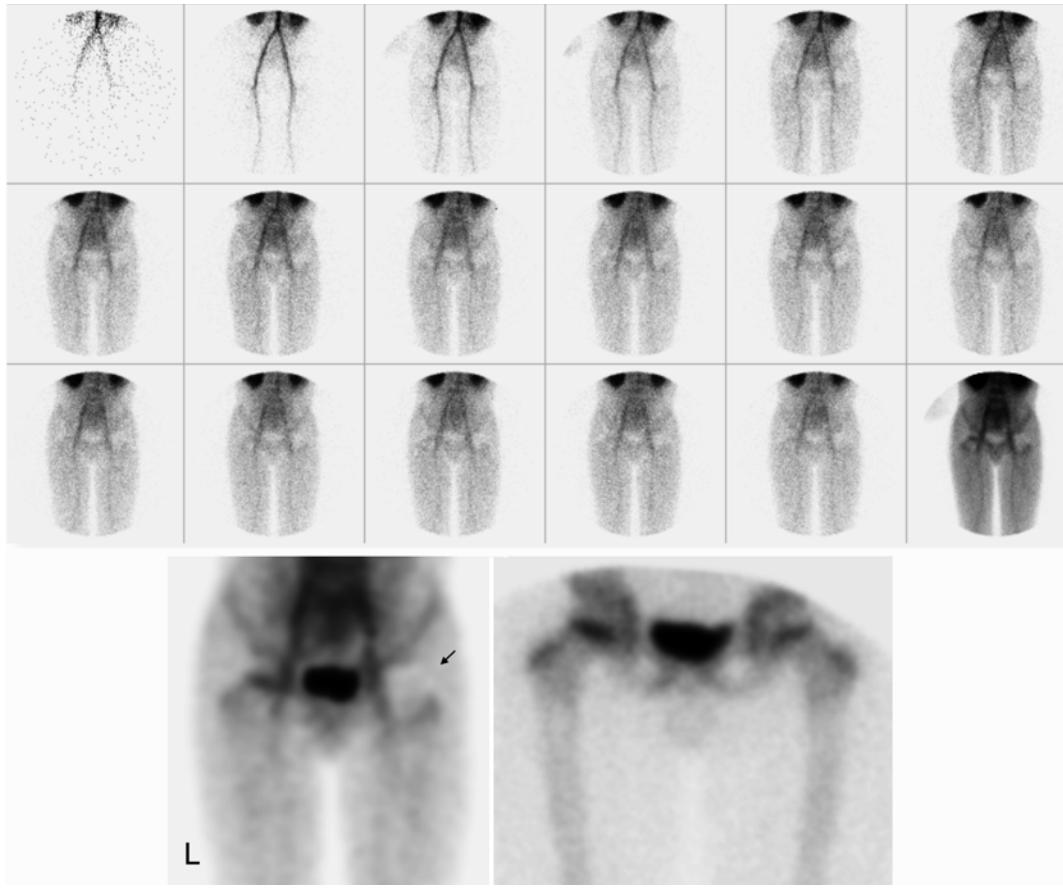

Fig. 15.6 Left hip effusion. The radionuclide angiogram reveals that left hip effusion is seen as absent tracer concentration in the region of the right hip (*top*). The tissue image (*left lower image*) shows decreased tracer concentration in the region of the left hip (*arrow*). The skeletal phase image (*right lower image*) shows that the left femoral head perfusion is preserved

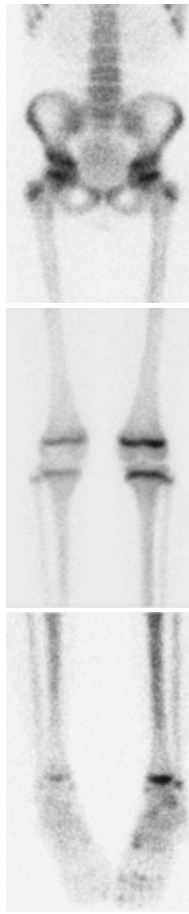

Fig. 15.7 An 8-year-old female with right leg pain for a week after a fall with twisting of her right leg. MRI revealed no hip pathology. The patient was using crutches and did not put weight on her right leg. There is diffusely decreased uptake throughout the right lower extremity due to reduced overall flow with disuse. Conversely, the left leg that was supporting the patient's weight reveals relatively increased tracer uptake

protein bound during the first hour, 45 % at 3 h and 100 % at 24 h. Approximately 40 % of the administered activity is found in the urine in one hour to 60 % and 70 % at 4 and 24 h after injection, respectively [2, 3]. Usual administered doses are 0.2 mCi (7.4 MBq)/kg of body weight with a minimum total dose of 0.5 mCi (18.5 MBq) [4].

Technetium-99m-phosphates are also known to accumulate in soft tissue lesions prone to ischemia and/or microcalcification such as in neuroblastoma, stroke, metastatic osteosarcoma, myocardial infarction, functional asplenia, muscle trauma, myositis ossificans, necrotizing enterocolitis, and hyperparathyroidism (Fig. 15.10).

Fluorine-18 Sodium Fluoride

Fluorine-18 sodium fluoride was recognized as an excellent skeletal imaging agent several decades ago [5]. Two principal factors are responsible for the increasing use of ^{18}F-NaF skeletal PET. One is due to the improved distribution of ^{18}F-labeled radiotracers that had been paved by the wide use of FDG. Therefore, commercially available ^{18}F-NaF is widely available at the present time. The other important factor is the development and wide installed base of modern PET and PET/CT scanners [6–8].

After intravenous administration, ^{18}F-NaF is rapidly cleared from the plasma by a biexponential mode. The first phase has a half-time of 0.4 h, and the second phase has a half-time of 2.6 h. Essentially all the ^{18}F-NaF that is delivered to bone by the blood is retained in the bone. One hour after administration of ^{18}F-NaF, only about 10 % of the injected dose remains in blood. Fluorine-18 sodium fluoride diffuses through capillaries into extracellular fluid space in bone, where it becomes bound by chemisorption at the surface of bone crystals, preferentially at sites of newly mineralizing bone. Deposition of ^{18}F in bone appears to be primarily a function of blood flow to, and the efficiency of the bone extracting ^{18}F-NaF. Fluorine-18 sodium fluoride does not appear to be permanently bound to serum proteins. In patients with normal renal function, 20 % or more of the fluorine ion is cleared from the body in the urine within the first 2 h after intravenous administration. A usual pediatric administered dose is 0.06 mCi (2.2 MBq)/kg to a maximum of 4 mCi (148 MBq). The usual minimum administered amount of this tracer is 0.5 mCi (18.5 MBq). Our experience with ^{18}F-NaF skeletal imaging goes back to the early 1970s, when for a period of time we used ^{18}F-NaF as a routine procedure. We obtained ^{18}F-NaF scintigraphy using a whole-body rectilinear scanner in patients of all ages (Fig. 15.11).

During the transition from ^{18}F-NaF to ^{99m}Tc-phosphates in 1974, we compared ^{18}F-NaF and pyrophosphate in children with neuroblastoma,

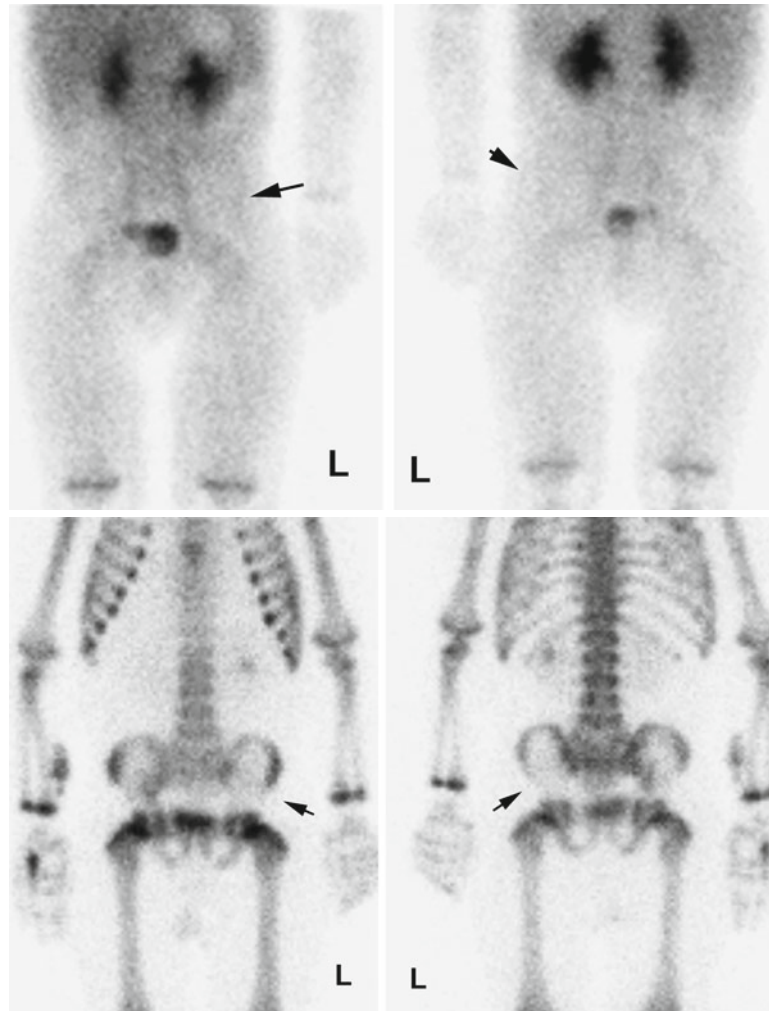

Fig. 15.8 Bone infarct. Images from a 5-year-old male with sickle cell disease. The tissue phase images show relatively reduced tracer accumulation in the region of the left hip (*top image*, *arrows*). The skeletal phase images reveal decreased-to-absent tracer uptake in the left iliac bone (*lower images*)

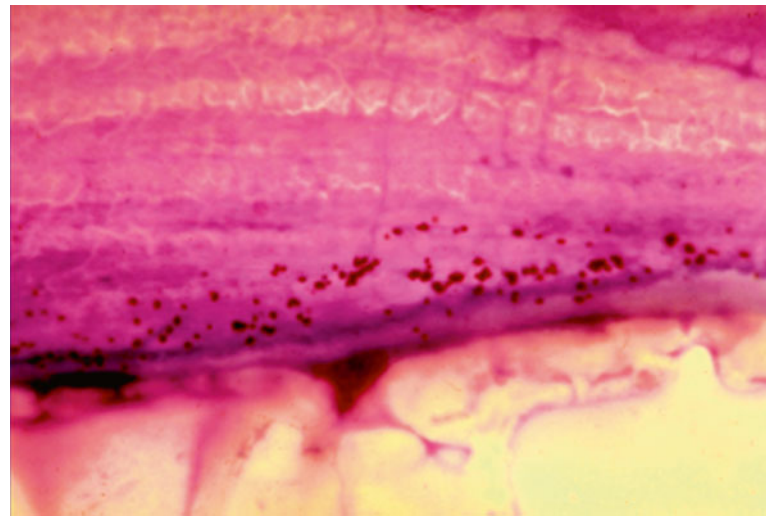

Fig. 15.9 Autoradiography of ^{99m}Tc-pyrophosphate from a human femur showing localization of silver granules just beneath osteoid

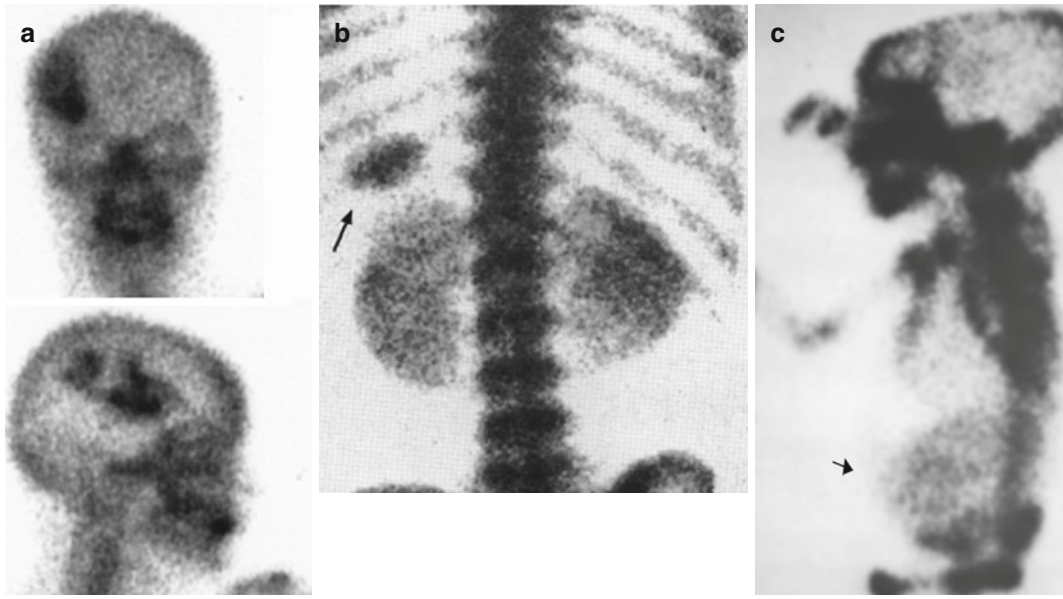

Fig. 15.10 Uptake of ^{99m}Tc-phosphates in soft tissues. (**a**) Stroke. (**b**) MDP in spleen (*arrow*) of patient with sickle cell disease. (**c**) Necrotizing enterocolitis in a newborn, intestine (*arrow*)

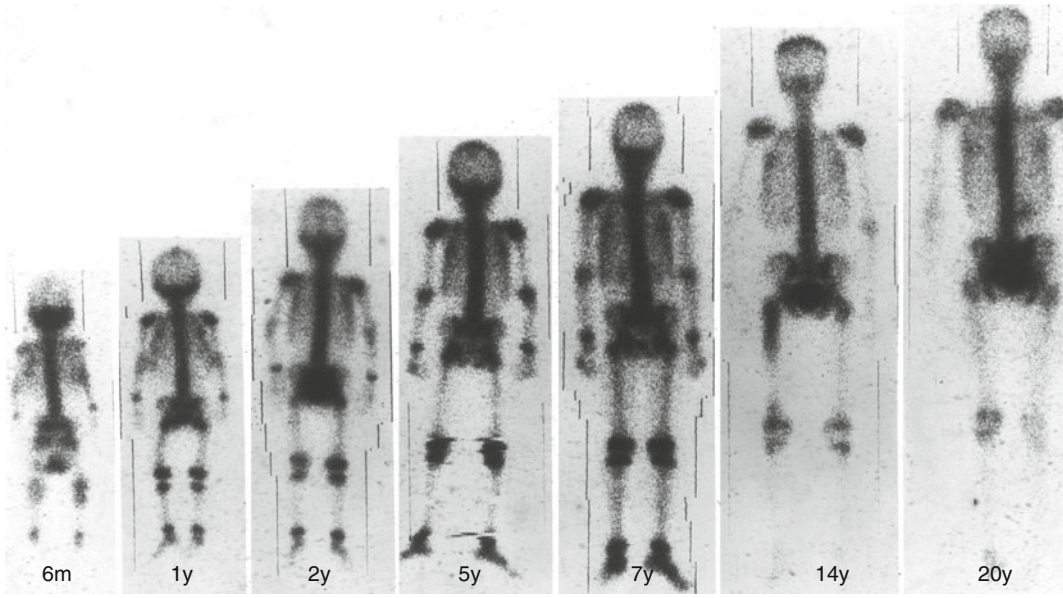

Fig. 15.11 ^{18}F-NaF whole-body scans in patients of all ages obtained with a whole-body rectilinear scanner

and the resulting patterns of distribution were similar [9]. Soon after technetium-labeled phosphates were introduced and made widely available, the use of ^{18}F-NaF decreased dramatically. The spatial resolution available with whole-body rectilinear scanners was rather poor compared with images obtained with modern PET systems (Fig. 15.12).

In addition to the agents mentioned above, other agents have been used for radionuclide skeletal imaging. These include ^{99m}Tc-sulfur colloid for bone marrow imaging, ^{18}F-FDG for tumors and infection/inflammation, ^{99m}Tc-HMPAO-labeled white blood cells for infection, and ^{201}Tl-chloride for tumor imaging.

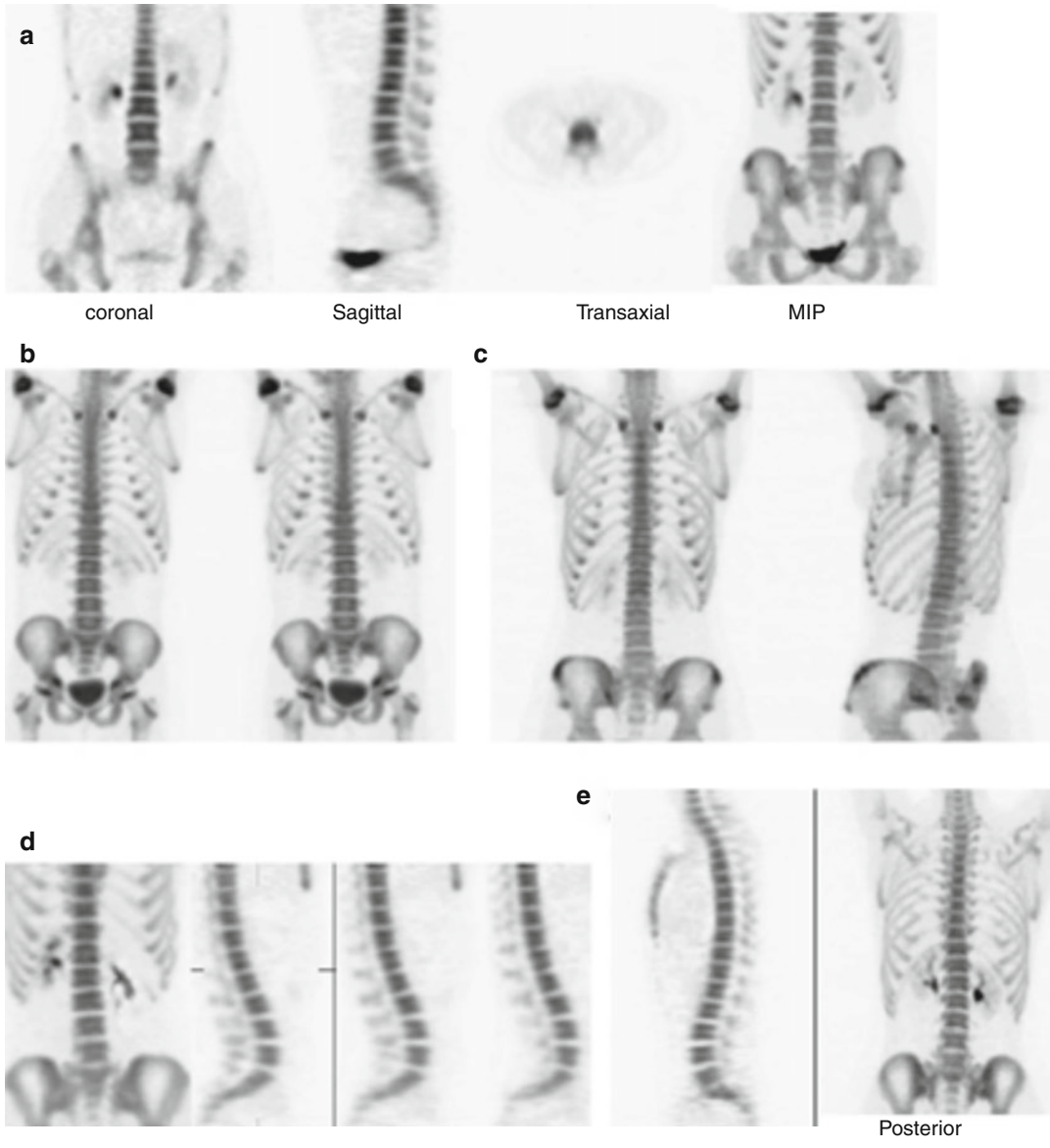

Fig. 15.12 Normal skeletal ^{18}F-NaF PET in patients aged 5 years (**a**), 11 years (**b**), 15 years (**c**), 19 years (**d**), and 30 years (**e**). Pattern of ^{18}F-NaF uptake in skeleton is similar to pattern seen with more familiar ^{99m}Tc-labeled diphosphonate bone scans and illustrates changes that occur with maturation of skeleton (Reproduced with permission by Grant et al.)

Imaging with ^{99m}Tc-MDP

Patient Preparation: The patient should be encouraged to drink plenty of fluids before scanning. No other preparation is needed, except to let the patient and caregivers know how long the entire procedure will take so that appropriate scheduling arrangements can be made. In the hands of well-trained and experienced technologists, patients do not need to be sedated for ^{99m}Tc-MDP scintigraphy. Small patients may need sedation for SPECT. If possible, patients should be asked to void before imaging. Examination of the pelvic region may be limited

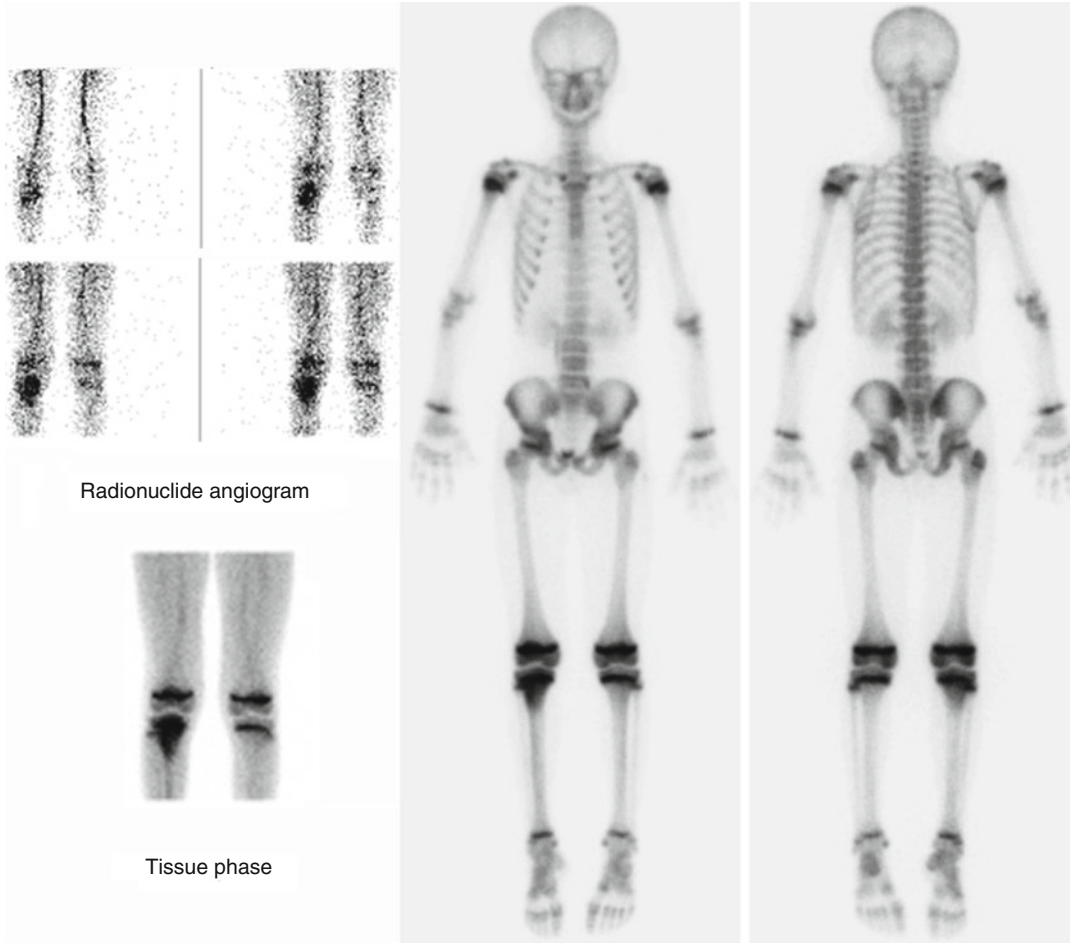

Fig. 15.13 A three-phase ^{99m}Tc-MDP bone scan in a teenager with osteomyelitis of the right proximal tibia. Increased blood flow to the area is seen on the radionuclide angiogram and increased localization in the right proximal tibia on the tissue phase image. The skeletal phase image also shows increased tracer uptake in the right proximal tibia

if the bladder is full of tracer. In some cases, bladder catheterization may be necessary in order to evaluate this region better.

Planar Imaging

Planar imaging may include one, two, or three phases (the "three-phase bone scan"): (a) radionuclide angiography, (b) immediate tissue phase images, and (c) skeletal images. The nuclear medicine physician may choose all three phases or would be satisfied by the skeletal phase only, and this will be determined by the patient condition and the diagnostic task at hand. Figure 15.13 shows a three-phase bone scan in a patient with osteomyelitis.

The three-phase approach is used when the clinical indication suggests infection, inflammation, or an aneurismal bone cyst. In cases of soft tissue inflammation without osteomyelitis, this can be revealed by radionuclide angiography and immediate phase images, but not on skeletal images if the bone itself has not been affected by increased blood flow, etc. The more time that elapses between tracer administration, the greater

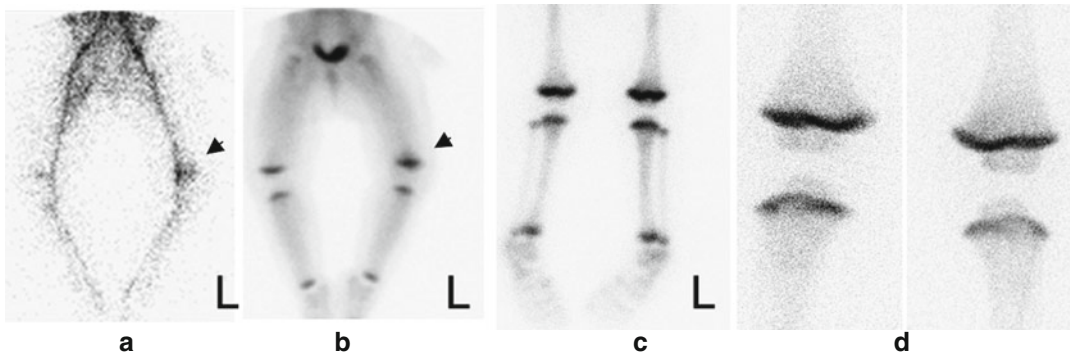

Fig. 15.14 Soft tissue inflammation, cellulitis. (**a**) Radionuclide angiogram shows increased blood flow to the region of the left knee. (**b**) Immediate tissue image shows a mild accumulation of tracer in the same region. (**c**) Skeletal phase image shows very mild increased uptake in the left distal femur and left proximal tibia. (**d**) Pinhole images do not reveal abnormal focal uptake in the bones of the left knee

the bone-to-background ratio. In some instances, images at approximately 24 h following tracer administration can be obtained and can be useful to further enhance the lesion-to-background difference ("the four-phase bone scan") [10].

Radionuclide Angiography

Radionuclide angiography is obtained immediately after the intravenous injection of the tracer as a dynamic study using a high-resolution collimator. Usual framing rates are from 1 frame per second to 1 frame per 0.5 s or on list mode with post-acquisition reframing. As the photon flux is relatively low given the amount of administered tracer, viewing is usually on summed 1.0 min images. Cinematic display is helpful for interpretation in some cases, and it should be used liberally. Images are usually acquired on a 128×128 format.

In patients with soft tissue inflammation without bone involvement, the radionuclide angiogram will show a focal region of increased tracer delivery corresponding to the region of inflammation (cellulitis). This may or may not be accompanied by bone involvement (Fig. 15.14).

The field of view for the angiogram is chosen based on the site of patient symptoms or the expected location of a lesion. However, if there is referred pain, the angiogram may miss the lesion. If this is suspected, it is useful to obtain tissue phase images of adjacent areas around the initial region of interest.

Immediate Tissue Phase Images

These images (also called "blood pool" images) are useful to assist in the detection of soft tissue lesions such as inflammation, infection, and soft tissue tumors. This information complements the radionuclide angiography and skeletal phase images allowing the differentiation of soft tissue only (cellulitis) versus a combination of soft tissue and skeletal abnormality (certain tumors). In some cases, it is useful to obtain a tissue phase image of the whole body. Since these images take a few minutes to obtain, tracer is already seen in the soft tissues and in bone, so the images are not purely reflecting the blood pool.

Skeletal Phase Images

Following the intravenous injection of ^{99m}Tc-MDP, skeletal phase images are usually obtained at 2, 3, or 4 h later. Techniques for planar skeletal

Fig. 15.15 A 2.5-year-old boy fell from bed 2 weeks ago and had normal x-rays of the ankle. The patient was treated with high-top sneakers. Patient did not improve. Skeletal scintigraphy reveals a curvi linear pattern of increased tracer uptake along the left tibia suggesting a spiral fracture. One week after the bone scan, follow-up radiographs confirmed a spiral fracture of the left tibia

phase imaging include multispot imaging, whole-body imaging, and pinhole magnification.

Multispot Imaging

Multispot imaging does not require patient sedation and can be relatively easily obtained with gentle immobilization in the hands of experienced technologists. Each image is obtained for approximately 500,000 counts on a 128×128 or 256×256 matrix format. Imaging symmetric parts of the body should be obtained based on the same imaging time so that right-left comparisons are easier to achieve. Multispot images are usually of higher spatial resolution than whole-body images (Fig. 15.15).

Whole-Body Imaging

These images give an overall view of tracer biodistribution throughout the body, which can be useful in the detection of focal lesions or help in elucidating certain systemic conditions. Some children, however, cannot or will not stay still for the duration of the whole-body scan (20–30 min) and may need to either be sedated or, alternatively, have the study done with multispot imaging. With the application of enhanced planar processing, it is possible to cut the whole-body scanning in half so that it is possible to obtain whole-body scans in some children without the need for sedation. Alternatively, with a normal scanning time, this method allows the administration of 50 % less radiopharmaceutical dose, thus reducing patient radiation exposure by half [11].

Pinhole Magnification Scintigraphy

Pinhole magnification is very useful for imaging small bones in children. The pinhole collimator provides images of very high resolution by spreading every point of the object over a larger area of the detector crystal. So, although the intrinsic spatial resolution of the gamma camera is not affected per se, the system's resolution is greatly improved so that objects in the 1–2 mm range can be imaged (see Chap. 27).

Pinhole magnification scintigraphy is useful in the evaluation of the hip (Figs. 15.4, 15.5, and 15.16), in the evaluation of small bones of the hands (Fig. 15.17) and feet, as well as in the characterization of osteoid osteoma (Figs. 15.18 and 15.19). The smaller the pinhole, the greater the system's spatial resolution. This is at the cost of sensitivity. The closer the pinhole collimator to the object, the higher the spatial resolution and the higher the sensitivity (Fig. 15.16).

In osteoid osteoma, the characteristic appearance on pinhole magnification is a focal and very intense region of tracer uptake corresponding to the area of the nidus. This is typically surrounded by an area of mild and diffuse tracer uptake. Planar imaging can detect the focal increased uptake, but the pinhole image shows a more characteristic diagnostic pattern.

Pinhole magnification scintigraphy can effectively assist before and during the surgical excision of osteoid osteomas anywhere in the body and especially in the central skeleton to ensure complete removal of the lesion. For this purpose, we use a mobile solid-state camera equipped

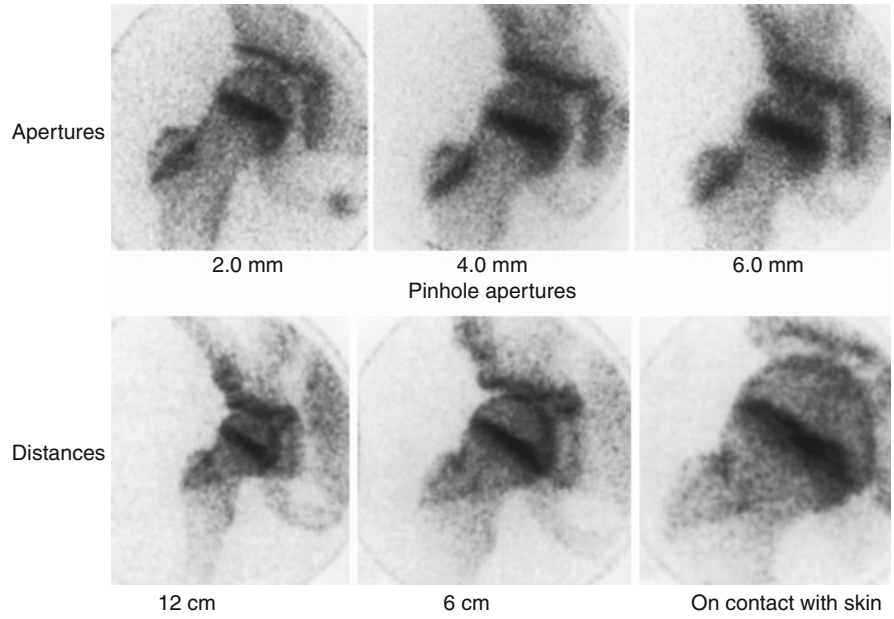

Fig. 15.16 Pinhole images of the hip showing the effects of different collimator apertures and different distances from the object

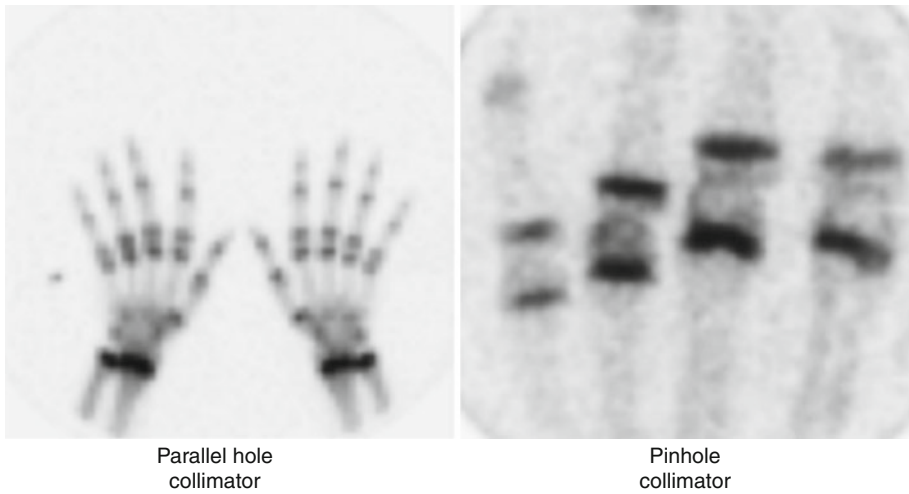

Fig. 15.17 A 10-year-old male with 2 months of pain and swelling in the region of the fourth left metacarpal phalangeal joint. The x-rays, CBC, and ESR were normal. The clinical question was osteomyelitis versus soft tissue process. The pinhole image (*right*) shows focally increased tracer uptake in the distal metacarpal bone adjacent to the joint

with a pinhole collimator, which is brought into the operating theatre. There, the camera is covered with sterile sheets, and the surgeon and the nuclear medicine physician collaborate using a series of images during the operation until there is assurance that no residual tissue corresponding to the osteoid osteoma is left behind. With this approach, the number of recurrent osteoid osteomas in our setting is virtually nonexistent (Fig. 15.19) [12–14].

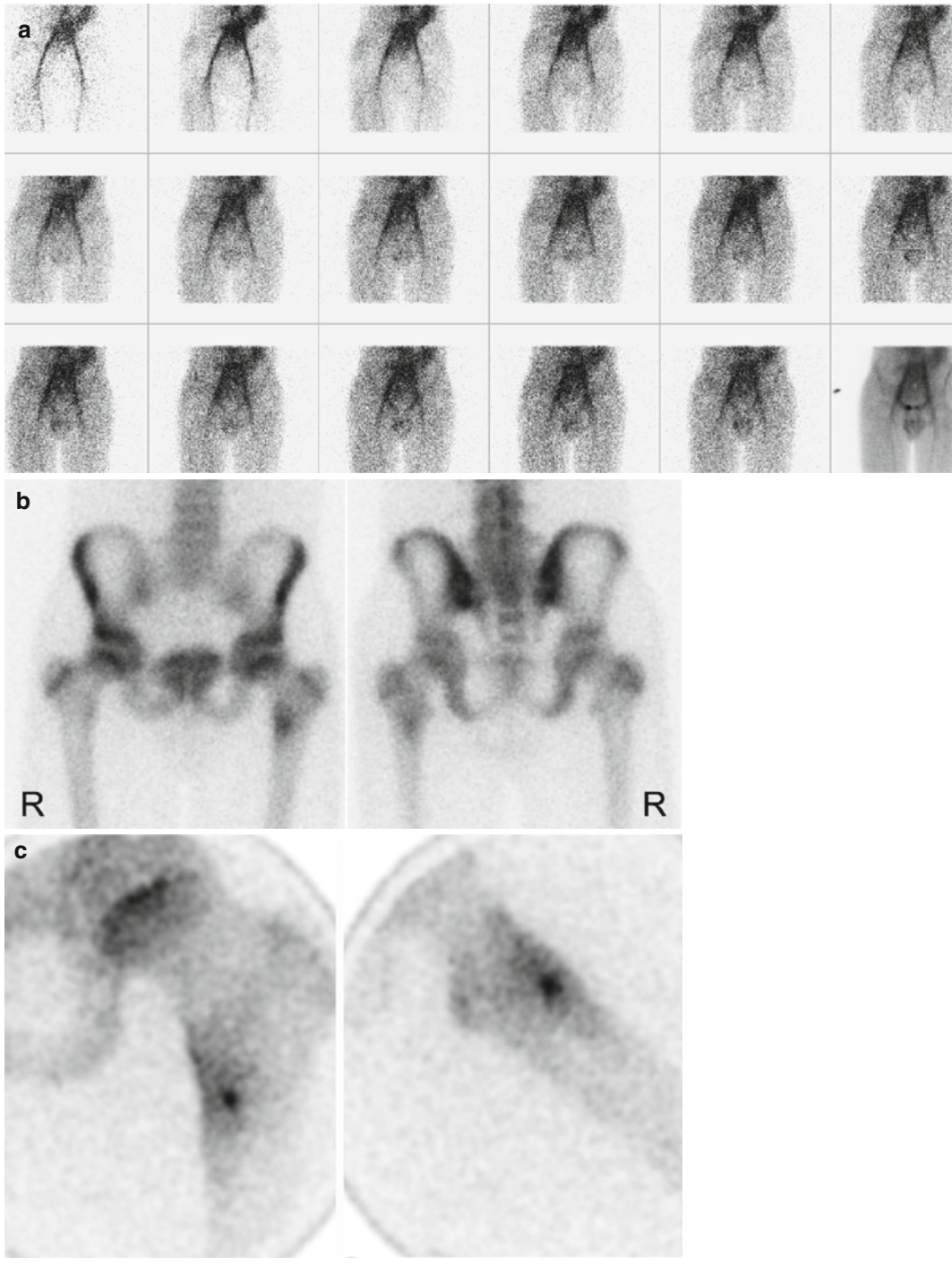

Fig. 15.18 Osteoid osteoma of the left proximal femur. Typical appearance where the radionuclide angiogram and the tissue phase image do not show an abnormality (**a**). The skeletal phase reveals focally increased tracer uptake in the region of the lesion (**b**). The pinhole image (**c**) shows the typical appearance of an osteoid osteoma: intense focal tracer uptake surrounded by a "cloud" of less intense and diffusely increased tracer uptake

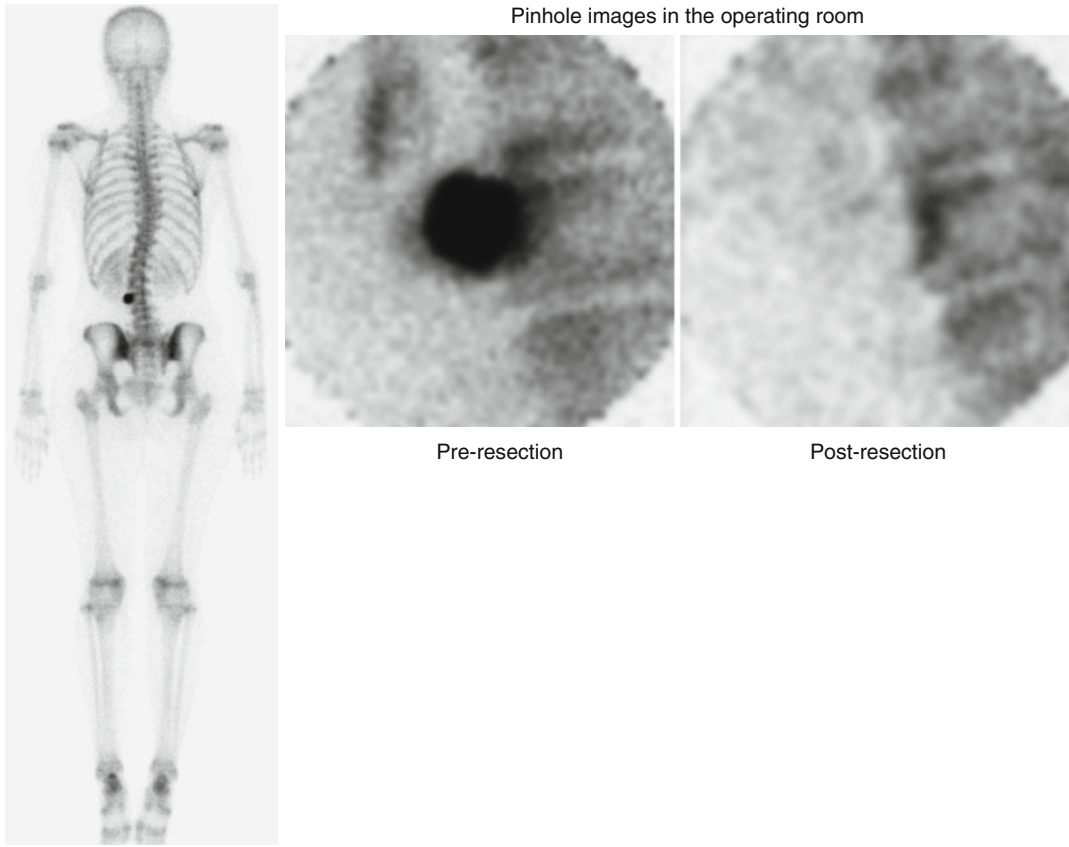

Fig. 15.19 Osteoid osteoma of the spine. The whole-body ^{99m}Tc-MDP bone scan shows an intense and well-localized region of increased uptake (*left panel*). Pinhole images obtained in the operating room show the osteoid osteoma as well as its absence after surgical resection (*right panel*)

The physical characteristics of the pinhole and pinhole magnification are discussed in greater detail in the chapter on Instrumentation and Image Processing. The closer the collimator is to the object, the greater the magnification and spatial resolution achieved.

SPECT

SPECT should be considered an integral tool in the routine evaluation of pediatric skeletal disorders including the investigation of the cause of back pain, fractures, osteoid osteoma, and tumors (Fig. 15.20). SPECT provides a three-dimensional image for improved localization and much higher contrast than planar imaging. SPECT has proven invaluable in the detection of skeletal abnormalities in young children and adolescents with back pain. SPECT is definitely superior to planar imaging for this diagnostic task, as planar imaging can frequently miss lesions that can be more readily detected on SPECT. Therefore, SPECT should be considered indispensable in the clinical setting of back pain. Most patients referred to our practice with back pain are young athletes. SPECT can detect early stress changes in the affected bones such as posterior elements, the spinous processes, and the pelvis (Fig. 15.21).

In addition to the role of SPECT in teenage athletes, we have seen stress changes in children younger than 10 years of age. In children of this age group complaining of back pain, skeletal SPECT reveals a high incidence of abnormal

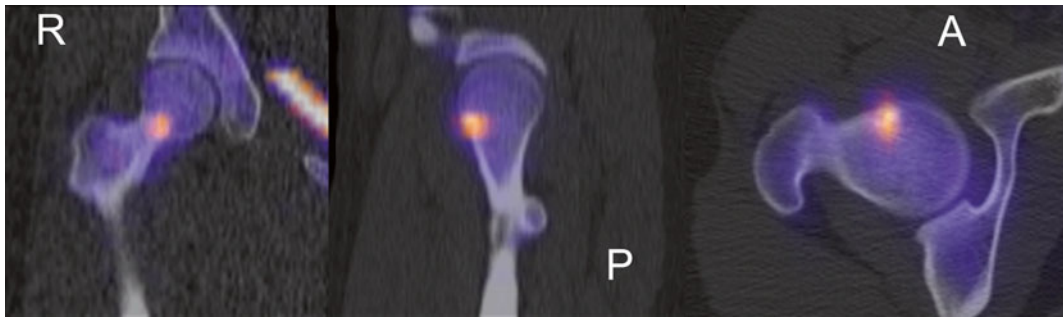

Fig. 15.20 Osteoid osteoma of the right femoral neck. ^{99m}Tc-MDP SPECT fused to a CT helps with the anatomic localization of the lesion

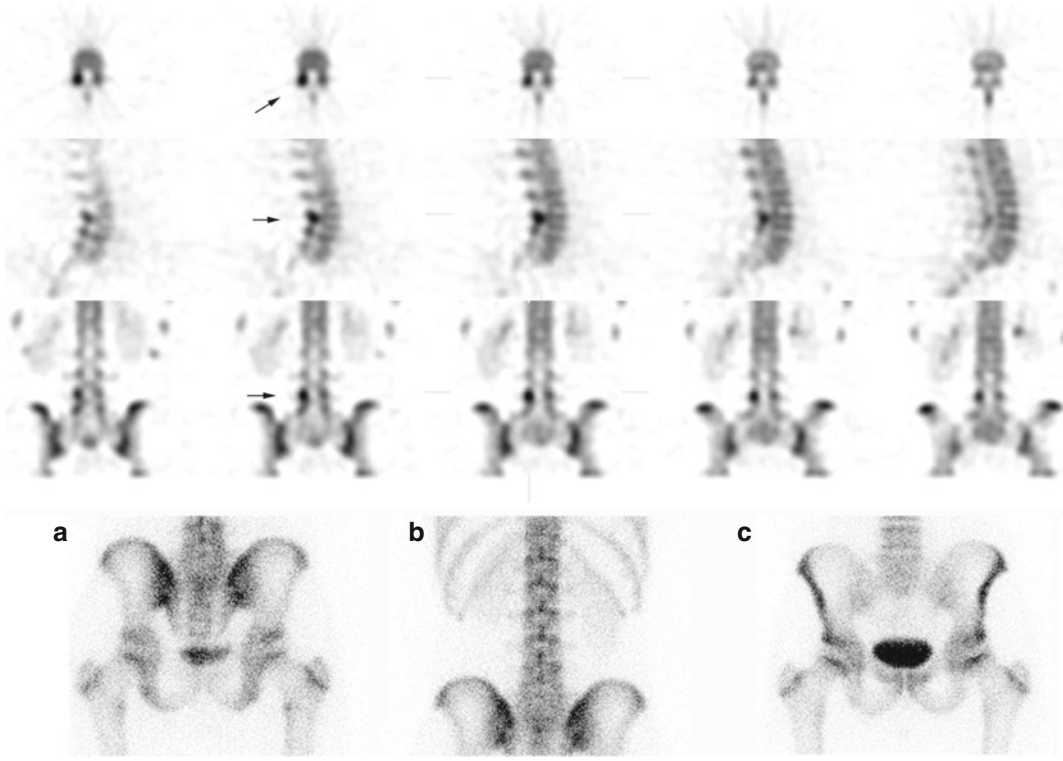

Fig. 15.21 A 17-year-old male experienced recent recurrence of back pain after high jumping, and running. Planar imaging (*bottom a–c)* does not reveal focal abnormality while the SPECT (*top*) clearly reveals focal increased tracer uptake at the level of left posterior element at L4 (*arrows*)

scintigraphic findings similar to those patterns seen in the older patients. In an early study, we found that in 50 patients younger than 10 years of age, approximately 20 % of the SPECT showed focal SPECT abnormalities in the spine (Fig. 15.22) [15].

Traditionally, pediatric SPECT is reconstructed with filtered back projection (FBP). Compared with newer reconstruction techniques, the spatial resolution and image quality with FBP are relatively low. Using advanced image processing such as *ordered subset expectation*

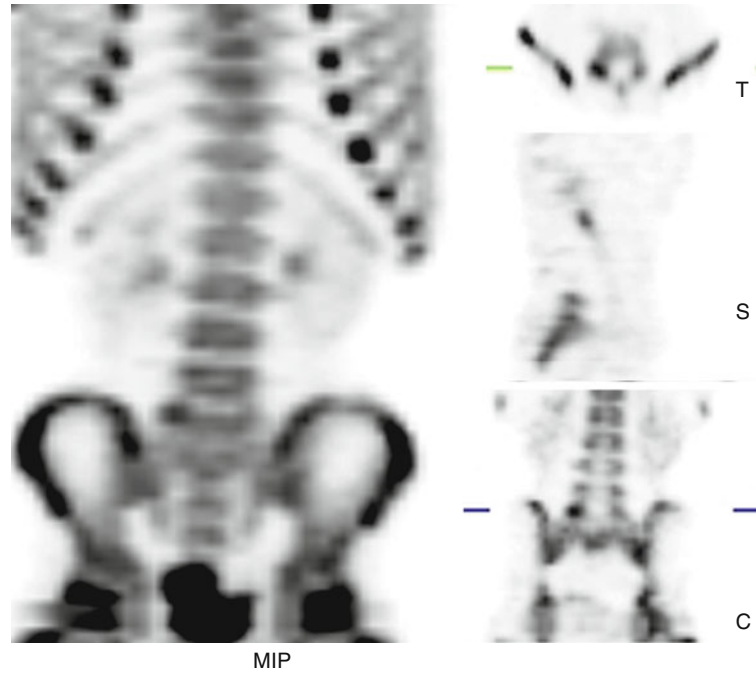

Fig. 15.22 SPECT with ^{99m}Tc-MDP. A 6-year-old male with mild levoscoliosis of the thoracolumbar spine and back pain. Radiographs at the times of the SPECT were unremarkable. SPECT shows focal intense tracer uptake in the posterior elements of the right L5. Later x-rays demonstrated grade I anterolisthesis of L5 on S1

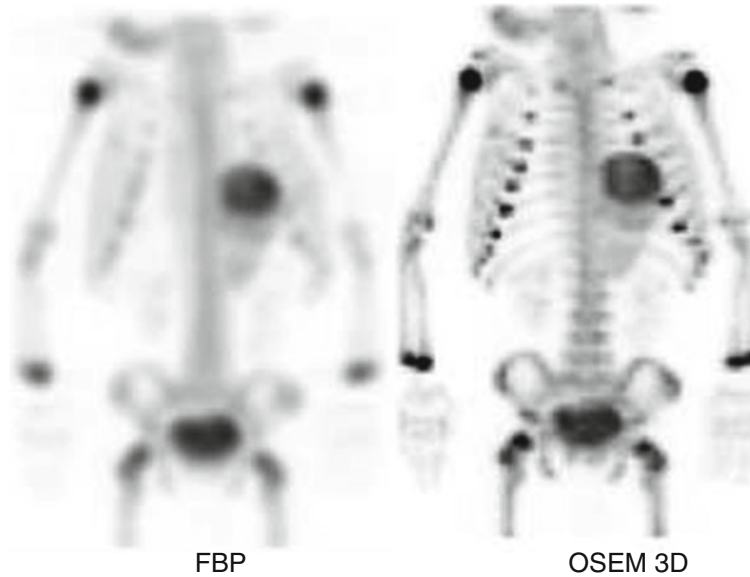

Fig. 15.23 Technetium-99m-MDP SPECT in neuroblastoma. OSEM-3D. Multiple-intensity projections (MIP) of a ^{99m}Tc-MDP SPECT from an 11-month-old boy with a right suprarenal mass later found to represent a neuroblastoma. On the left of the image is a conventional FBP reconstruction. The right image from the same acquisition was processed with OSEM-3D showing improvement in image quality

maximization iterative reconstruction with isotropic 3D resolution recovery (OSEM-3D) can significantly improve SPECT image resolution. At the same time, this method allows for a reduction of radiopharmaceutical administered dose and therefore patient radiation dose (Fig. 15.23). In addition, OSEM-3D allows for significant shorter image acquisition times, thus improving patient comfort and reducing patient motion as well. Depending on the patient's clinical need, it is possible to achieve a combination of gains in terms of improved resolution as well as in dose

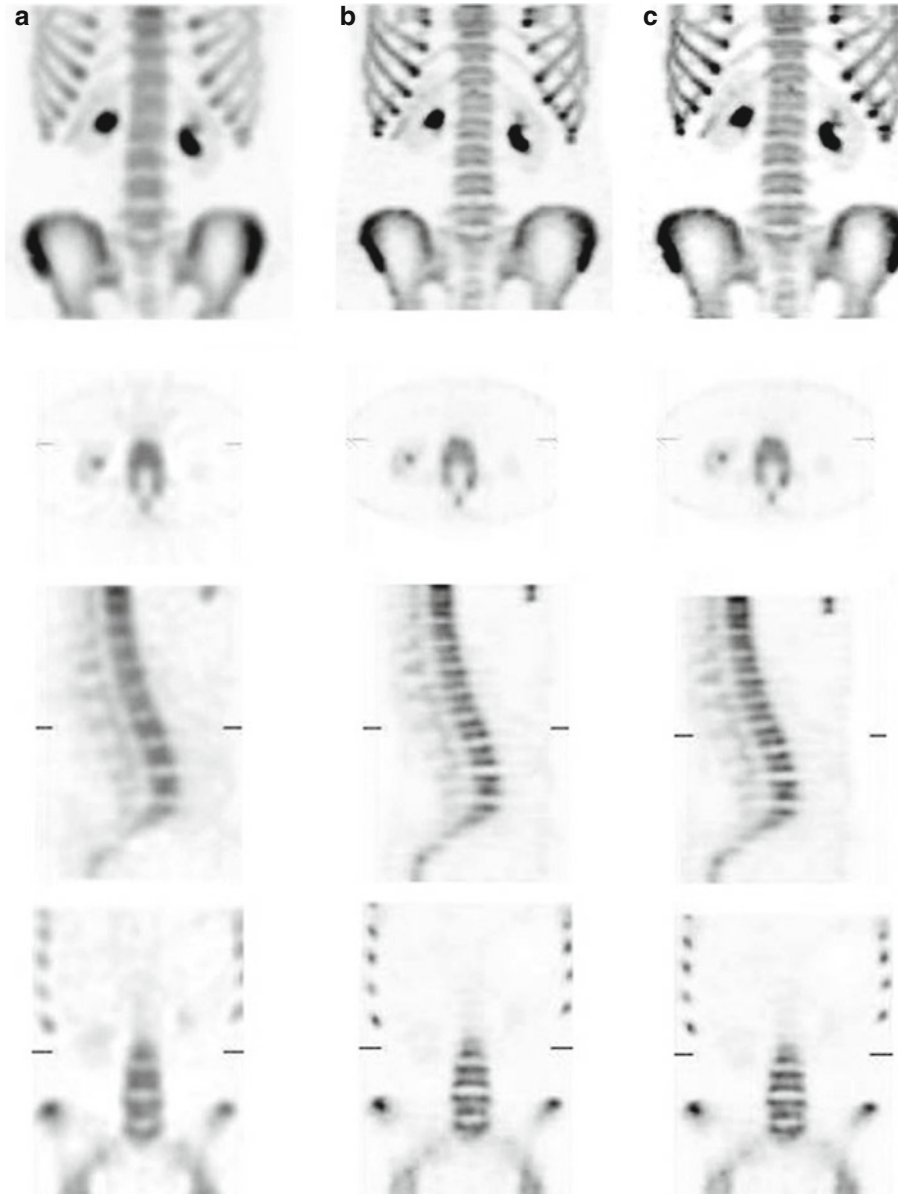

Fig. 15.24 Normal spine SPECT study reconstructed three different ways: (**a**) two-detector FBP at full tracer dose; (**b**) two-detector FBP reconstructed with OSEM-3D, also at the full tracer dose showing resolution improvement; and (**c**) one-detector FBP which corresponds to half the counts reconstructed with OSEM-3D. Observe that there is no significant difference between full dose and half dose with OSEM-3D. *Top row*: volume rendered images. *Second row*: transaxial images. *Third row*: sagittal images. Bottom row: coronal images (From Stansfield et al. [17], with permission)

reduction and scanning speed [16–18]. We have evaluated the use of OSEM-3D (Flash 3D, Siemens Medical Solutions) in patients undergoing ^{99m}Tc-MDP SPECT of the spine and found the results with OSEM-3D quite impressive compared to conventional SPECT reconstruction using filtered back projection (FBP) (Fig. 15.24).

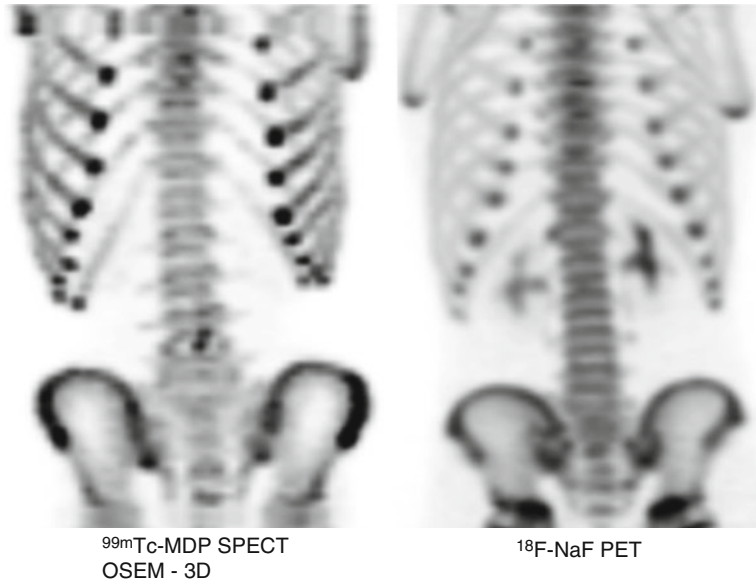

Fig. 15.25 Comparison of ^{99m}Tc-MDP SPECT reconstructed with OSEM-3D with resolution recovery (*left*) with ^{18}F-NaF PET (*right*) in two age-matched patients. The images appear very similar in terms of quality and spatial resolution

Fluorine-18 Sodium Fluoride PET

Characteristics of skeletal ^{18}F-NaF PET include the ability to obtain the images 0.5–1.0 h after the tracer administration, rather than the 15–30 min with ^{99m}Tc-MDP. Results can be available rapidly to be communicated to the referring physician. Patient schedule is more convenient, as the total time commitment for the patient is much less than with ^{99m}Tc-MDP SPECT. Also, the spatial resolution of PET is relatively high. However, total scanning time may be the same or, depending on the PET scanner and the volume imaged, longer than with SPECT. Tracer availability with ^{18}F-NaF is rather limited, while MDP is readily available at any time. With PET it is not easy to obtain a three-phase study as with single-photon studies. An equivalent to pinhole magnification is not available with ^{18}F-NaF PET. Also, one should consider advanced image processing of ^{99m}Tc-MDP SPECT such as OSEM-3D as a viable alternative (Fig. 15.25).

For ^{18}F-NaF PET, no patient preparation is required. However, if possible, the patient should be well hydrated before the injection in order to promote urinary elimination of the tracer for imaging. The patient is injected with ^{18}F-NaF intravenously. It is possible to obtain adequate skeletal PET following oral administration of ^{18}F-NaF. However, the time for imaging for the oral route should be approximately one hour after administration to allow for a slower oral absorption compared to the intravenous route. Also, it is important to note that some of the tracer may remain in the GI tract at the time of imaging. Oral administration should be considered in children that do not have easy intravenous access or when the region to be imaged is outside the abdomen. Imaging can begin at 15–30 min following intravenous tracer injection. If possible, the patient is instructed to void just before imaging. In some patients, it is necessary to use sedation for PET imaging. Our studies are acquired in 3D mode. The field of imaging depends on the clinical indication. For back pain, we image the lower thoracic, lumbar, and pelvic region, but this can be extended as needed according to the patient's symptoms. In oncology patients, imaging is from head to toes. For the assessment of non-accidental trauma, imaging is also from head to toes. Assessment of the pelvic region can be compromised if the bladder is full of tracer. In these cases, the patient should be asked to void if possible and a repeat image should be obtained. In certain cases, it may be necessary to place a bladder catheter to clear the bladder of activity before reimaging.

The skeletal PET scan is viewed as rotating MIP images and by evaluating slices in three dimensions. If the scanner has no CT, in some cases, it is useful to fuse the PET image with a preexisting CT to aid in lesion localization. In our experience, this is not frequently needed. Of course, if a PET/CT instrument is used, anatomic localization of lesions is readily available in all cases. As in the case of skeletal imaging with ^{99m}Tc-MDP, most lesions will reveal increased tracer uptake regionally or locally, depending on the diagnosis. Certain lesions such as vascular tamponade, aseptic necrosis, and infarcts may appear devoid of activity.

PET images show relatively high resolution compared to conventional SPECT reconstructed with filtered back projection (FBP). However, as mentioned earlier, recent application of iterative reconstruction with 3D resolution recovery has proven to improve skeletal SPECT at spatial resolutions closer to that of PET and with lower radiation exposure to the patient.

References

1. Tilden RL, Jackson Jr J, Enneking WF, DeLand FH, McVey JT. 99m Tc-polyphosphate: histological localization in human femurs by autoradiography. J Nucl Med. 1973;14(8):576–8.
2. Subramanian G, McAfee JG, Bell EG, Blair RJ, O'Mara RE, Ralston PH. 99m Tc-labeled polyphosphate as a skeletal imaging agent. Radiology. 1972; 102(3):701–4.
3. Subramanian G, McAfee JG, Blair RJ, Kallfelz FA, Thomas FD. Technetium-99m-methylene diphosphonate–a superior agent for skeletal imaging: comparison with other technetium complexes. J Nucl Med. 1975;16(8):744–55.
4. Gelfand MJ, Parisi MT, Treves ST. Pediatric radiopharmaceutical administered doses: 2010 North American consensus guidelines. J Nucl Med. 2011;52(2):318–22.
5. Blau M, Nagler W, Bender MA. Fluorine-18: a new isotope for bone scanning. J Nucl Med. 1962;3:332–4.
6. Grant FD, Fahey FH, Packard AB, Davis RT, Alavi A, Treves ST. Skeletal PET with 18F-fluoride: applying new technology to an old tracer. J Nucl Med. 2008; 49(1):68–78.
7. Grant FD, Drubach LA, Treves ST. 18F-Fluorodeoxyglucose PET and PET/CT in pediatric musculoskeletal malignancies. PET Clin. 2010;5(3):349–61.
8. Grant FD, Laffin SP, Davis RT, Drubach LA, Fahey FH, Treves ST. Skeletal PET with F-18 sodium fluoride as an alternative to Tc-99m bone SPECT in children. Pediatr Radiol. 2010;40(4):538.
9. Rosenfield N, Treves S. Osseous and extraosseous uptake of fluorine-18 and technetium-99m polyphosphate in children with neuroblastoma. Radiology. 1974;111(1):127–33.
10. Alazraki N, Dries D, Datz F, Lawrence P, Greenberg E, Taylor Jr A. Value of a 24-hour image (four-phase bone scan) in assessing osteomyelitis in patients with peripheral vascular disease. J Nucl Med. 1985;26(7): 711–7.
11. Mawlawi O, Yahil A, Vija H, Erwin W, Macapinlac H. Reduction in scan duration or injected dose in planar bone scintigraphy enabled by Pixon(R) postprocessing. Soc Nucl Med Annu Meet Abstr. 2007;48(Meeting Abstracts 2):13P-b.
12. Roach PJ, Connolly LP, Zurakowski D, Treves ST. Osteoid osteoma: comparative utility of high-resolution planar and pinhole magnification scintigraphy. Pediatr Radiol. 1996;26(3):222–5.
13. Taylor GA, Shea N, O'Brien T, Hall JE, Treves ST. Osteoid osteoma: localization by intraoperative magnification scintigraphy. Pediatr Radiol. 1986;16(4): 313–6.
14. Blaskiewicz DJ, Sure DR, Hedequist DJ, Emans JB, Grant F, Proctor MR. Osteoid osteomas: intraoperative bone scan-assisted resection. Clinical article. J Neurosurg Pediatr. 2009;4(3):237–44.
15. Sokol L, Zurakowski D, D'Hemecourt P, Micheli L, Treves ST. Back pain in children less than 10 years of age: high incidence of abnormalities detected on skeletal single photon emission computed tomography (SPECT). Pediatr Radiol. 2010;40(4):539.
16. Sheehy N, Tetrault TA, Zurakowski D, Vija AH, Fahey FH, Treves ST. Pediatric 99mTc-DMSA SPECT performed by using iterative reconstruction with isotropic resolution recovery: improved image quality and reduced radiopharmaceutical activity. Radiology. 2009;251(2):511–6.
17. Stansfield EC, Sheehy N, Zurakowski D, Vija AH, Fahey FH, Treves ST. Pediatric 99mTc-MDP bone SPECT with ordered subset expectation maximization iterative reconstruction with isotropic 3D resolution recovery. Radiology. 2010;257(3):793–801.
18. Vija AH, Hawman EG, Engdahl JC. Analysis of a SPECT OSEM reconstruction method with 3D beam modeling and optional attenuation correction: phantom studies. Paper presented at Nuclear Science Symposium Conference Record, IEEE; 19–25 Oct 2003.